AIMS Mathematics, 8(10): 23472–23499.
DOI:10.3934/math.20231193
Received: 27 May 2023
Revised: 19 July 2023
Accepted: 24 July 2023
Published: 27 July 2023

http://www.aimspress.com/journal/Math

Research article

A class of generalized quadratic B-splines with local controlling functions

Qi Xie and Yiting Huang*

School of Mathematics, South China University of Technology, Guangzhou 510641, China

* **Correspondence:** Email: 201930220067@mail.scut.edu.cn.

Abstract: In this work, a class of generalized quadratic Bernstein-like functions having controlling functions is constructed. It contains many particular cases from earlier papers. Regarding the controlling functions, sufficient conditions are given. Corner cutting algorithms and the accompanying quadratic Bézier curves are discussed. A class of generalized quadratic B-splines possessing controlling functions is proposed. Some important properties for curve and surface design are proved. Sufficient conditions for C^2 continuity, C^3 continuity and C^n continuity are also given. Some applications of the constructed B-splines in $\mathbb{R}^2$ and $\mathbb{R}^3$ are presented, which show the ability to adjust the shape of the curves flexibly and locally. These applications show that generalized quadratic B-splines can be easily implemented and serve as an alternative strategy for modeling curves.

Keywords: quadratic Bernstein-like functions; quadratic B-splines; extended Chebyshev spaces; C^n continuity; curve design
Mathematics Subject Classification: 41A15

1. Introduction

Curve and surface design is a basic subject within Computer Aided Geometric Design (CAGD). Parametric curves and surfaces are usually represented by linear combinations of control points and basis functions, and the construction of basis functions which are normalized, nonnegative and totally positive, have received much attention.

In 1946, the theory of B-splines was first proposed by Schoenberg. In 1962, Bézier curves were proposed by French engineer Pierre Bézier. Bézier curves have an intuitive geometric representation, but also have strong integrity and weak local adjustment ability, see [1–3]. To adjust the curve shape, many methods have been presented subsequently. In 1972, de Boor gave a recursive algorithm for B-spline basis in [4]. The B-spline inherits all strengths of the Bézier methods and it overcomes the disadvantage that the Bézier curve can only be adjusted as a whole. In 1975, the rational B-spline was proposed by Versprille in [5] to overcome the problem that the B-spline method cannot accurately

represent the quadratic curve surface.

Blossoming is essential to construct splines, which is initially introduced in [6]. In [7], based on previous research on Chebyshev spaces, a blossom can be yielded by the bilinear form, which has an extension to the Chebyshev splines. In [8], Mazure further applied the main properties of blossoms in quasi-Chebyshev space, and proposed the requirements of blossom for spline by studying variable degree polynomial splines with connection matrices. In [9], according to Mazure, the blossom in spline space makes optimal bases possible automatically. In [10], the approximation power, the existence of a normalized B-basis and the assumptions required for the structure of a degree-raising process for some space were studied. In [11], Mazure provided new insights into specific conditions of the quasi extended Chebyshev spaces, and addressed the dimension elevation process in more general spaces. In [12], a new spline space with general tension properties was studied, which was profitable to use to construct shape-preserving curves.

Since Bernstein basis and B-spline basis do not have shape parameters, the shape of their corresponding curves is only determined by their control points. Therefore, we have to adjust the curve shape through modifying the control points, which brings inconvenience to the geometric design. In addition, as parametric curves defined by polynomials, Bézier curves and B-splines cannot represent other conic curves than parabolas.

In order to solve the above deficiencies, in recent years, many basis functions with shape parameters similar to Bernstein functions and B-splines in different function spaces have been proposed. By incorporating the shape parameter in the classical Bernstein basis, Han Xuli obtained a class of quadratic polynomial functions in [13]. Xie and Hong developed a method of generating quadratic B-spline curves having several parameters in [14]. In [15], Yan and Liang proposed a kind of quadratic $\alpha\beta$-Bernstein functions and the accompanying B-splines having local parameters.

The common point of the above work is that the curve properties are similar to those of quadratic Bézier curves, such as endpoint properties, symmetry, convex hull and geometric invariability. Moreover, by adjusting the parameters, the curves on both sides of the Bézier curve can be generated, which breaks through the approximation of the general Bézier curve to the control polygon. However, there is still the problem of being unable to represent conic sections other than parabolas. In 2002, Han presented a set of C^1 continuous quadratic trigonometric spline bases with one parameter in [16]. Wu proposed a kind of new quadratic trigonometric Bernstein functions having parameters in [17]. With the shape parameters, the trigonometric polynomial curves can yield tight envelopes for the quadratic B-spline curves and can be closer to the given control polygon than the quadratic B-spline curves. In [18], Han further extended the spline basis from one parameter in [16] to two local shape parameters, which serve as local control tension and local control bias in the curves. This work made the basis function more flexible to adjust curve shape locally. In 2003, Han provided the C^2 continuous quadratic trigonometric polynomial curves in [19]. Afterwards, he extended it to that with one local parameter and provided additional methods of adjusting curves in [20]. In 2013, a G^2 and C^2 rational quadratic Bernstein basis with two parameters was given by Bashir and Abbas in [21]. In 2015, Yan constructed a kind of quadratic hyperbolic polynomial curve with parameters called the H-Bézier curve in [22]. In [23], the problem of assigning tangents to a sequence of points in $\mathbb{R}^3$, compatible with a G^1 piecewise-PH-cubic spline interpolating those points, is also briefly addressed. The performance of these methods, in terms of overall smoothness and shape-preservation properties of the resulting curves, is illustrated by a selection of computed examples. This curve has shape

adjustability and can represent a hyperbola. In 2016, least squares approximation of Bézier coefficients with factored Hahn weights provided the best constrained polynomial degree reduction with respect to the Jacobi L_2-norm in [24]. This work extended many previous findings concerning polynomial degree reduction. In [25], González and his coauthors presented various designs and models of C^2 algebraic-trigonometric Pythagorean hodograph splines with shape parameters.

The present paper proposes a new generalized quadratic Bernstein-like function in space $T_{u,v} := \text{span}\{1, u(t), v(t)\}$, whose controlling functions $u(t)$ and $v(t)$ have clear geometric control significance for the generated curved surface shape. The optimal totally positive basis proposed in this paper includes many special cases with different shape functions, which are stated in [13–22] in detail. This newly-proposed generalized quadratic Bernstein-like function has good properties and a wide range of usage. To facilitate the construction of new basis functions, some simplified conditions for construction are proposed. In view of these simplified conditions, three typical cases of different controlling functions $u(t)$ and $v(t)$ are verified, and the accompanying applications in these cases are presented. Furthermore, some additional simplified construction conditions are proposed to enable the curve to achieve higher-order continuity. Specific examples are verified and the corresponding applications are given.

The rest of the article is separated into the following parts. Section 2 introduces the materials and methods that we mainly use. Section 3 presents how we construct the generalized quadratic Bernstein-like functions and their properties, followed by three typical examples. The accompanying quadratic Bézier curves and the corner cutting algorithms are provided. Section 4 introduces the construction and some properties of generalized quadratic B-splines, and the extra conditions that ensure the controlling functions have higher-order continuity. Section 5 shows the definition and applications of the corresponding curves. Futhermore, we analyse the relationship between curves and controlling functions. We also propose continuity conditions. Section 6 discusses and compares the generalized quadratic B-splines against classical splines. Section 7 gives the conclusion.

2. Materials and methods

2.1. Extended Chebyshev space and blossom theory

Herein, a brief introduction of Chebyshev space and Extended Completed Chebyshev space is given. The geometry approach of blossom theory is introduced, including a de Casteljau algorithm. These will be further applied in basis and curve construction. More details are stated in [8, 11, 26–30].

Definition 1. *Given an interval $I = [a, b]$, $U_{n+1} := (u_0, u_1, \cdots, u_n)$ is said to be an (n+1)-dimensional Extended Chebyshev space (EC space) on I if any nonzero element of U_{n+1} has at most n zeros (counted with multiplicities) in I. It is said to be an Extended Completed Chebyshev space (ECC space) on I if there exists positive weight functions $w_i \in C^{n-i}(I)$, $i = 0, 1, \cdots, n$, satisfying*

$$\begin{cases} u_0(t) = w_0(t), \\ u_1(t) = w_0(t) \int_a^t w_1(t_1)\mathrm{d}t_1, \\ u_2(t) = w_0(t) \int_a^t w_1(t_1) \int_a^{t_1} w_2(t_2)\mathrm{d}t_2\mathrm{d}t_1, \\ \quad\quad \vdots \\ u_n(t) = w_0(t) \int_a^t w_1(t_1) \int_a^{t_1} w_2(t_2) \cdots \int_a^{t_{n-1}} w_n(t_n)\mathrm{d}t_n \cdots \mathrm{d}t_1. \end{cases} \tag{2.1}$$

Remark 1. *On $I = [a, b]$, an EC space is an ECC space.*

The relevant proof is provided in [31].

Blossom is a powerful method for studying polynomial freeform surfaces, which is stated in detail in [6]. The French scholar Mazure has conducted in-depth and systematic research on the geometry approach of blossom, and has achieved rich theoretical and application results in [8, 11, 26–28, 32–34]. Next, we introduce the geometry approach of blossom theory.

Definition 2. *Let $\mathcal{E} \subset C^{n-1}$ be an (n+1)-dimensional Quasi Extended Chebyshev space of real valued functions defined on a closed bounded interval I. Let $\Phi_1, \cdots, \Phi_n \subset \mathcal{E}$, such that $(1, \Phi_1, \cdots, \Phi_n)$ is a basis of $\mathcal{E}$. The function $\Phi := (\Phi_1, \cdots, \Phi_n)$:$I \to \mathbb{R}^n$ so defined will be called the generating function, $\Phi \in C^{n-1}(I)$. For all integer $i \leq$ n-1 and $x \in I$, we have*

$$Osc_i\Phi(x) := \left\{\Phi(x) + \lambda_1\Phi'(x) + \cdots + \lambda_i\Phi^{(i)}(x) \mid \lambda_1, \cdots, \lambda_i \in \mathbb{R}\right\}. \tag{2.2}$$

For positive integer $\mu_1, \cdots, \mu_r$ whose sum is n, and distinct points $a_1, \cdots, a_r$, the blossom of generating function $\Phi(x)$ is defined as the intersection of osculating planes. Thus, $\varphi := (\varphi_1, \cdots, \varphi_n) : I^n \to \mathbb{R}^n$ satisfies

$$\{\varphi(x_1, \cdots, x_n)\} := \bigcap_{i=0}^{n} \mathrm{Osc}_{n-\mu_i}\Phi(a_i), \tag{2.3}$$

where $(x_1, \cdots, x_n) = (a_1^{[\mu_1]}, \cdots, a_r^{[\mu_r]}) := (\underbrace{a_1, \cdots, a_1}_{\mu_1}, \cdots, \underbrace{a_r, \cdots, a_r}_{\mu_r})$.

For any $(a, b) \in I^2$, the value of blossom $\Pi_i(a, b) := \varphi(a^{[n-i]}, b^{[i]})$, $i = 0, \cdots, n$, is called the Chebyshev-Bézier points of the blossom φ at the point (a, b). Obviously, we have

$$\begin{aligned} &\Pi_0(a, b) = \Phi(a), \qquad \Pi_n(a, b) = \Phi(b), \\ &\{\Pi_i(a, b)\} = \mathrm{Osc}_i\Phi(a) \cap \mathrm{Osc}_{n-1}\Phi(b), \quad 1 \leq i \leq n-1. \end{aligned} \tag{2.4}$$

Remark 2. *The three important properties of blossom theory are as follows:*

(1) Symmetry;

(2) Pseudo affine;

(3) Diagonal property.

Definition 3. *We can define a kind of de Casteljau algorithm at the point $\Pi_i(a, b)$ according to the three properties of blossom when $a \neq b$. We can derive from the n-th step of the algorithm that the value of the blossom φ of the convex combination of the point $\Pi_i(a, b)$ is*

$$\Phi(x) = \sum_{i=0}^{n} B_i^{(a,b)}(x)\Pi_i(a, b), \ \sum_{i=0}^{n} B_i^{(a,b)}(x) = 1, \ x \in I. \tag{2.5}$$

Knowing that $(1, \Phi_1, \cdots, \Phi_n)$ is a basis of $\mathcal{E}$, and the osculating plane of the generating function Φ can span the whole $\mathbb{R}^n$, we have the Chebyshev-Bézier points $\Pi_i(a, b)$ are affinely independent, $i = 0, \cdots, n$. Thus, $B_i^{(a,b)}(x)$, $i = 0, \cdots, n$, form a basis of $\mathcal{E}$, which is called the quasi Bernstein basis associated with the point (a, b).

3. Generalized quadratic Bernstein-like functions

3.1. Construction and properties

In the following part, when $t \in [0, 1]$, we will use the generalized quadratic function space $T_{u,v} := \text{span}\{1, u(t), v(t)\}$, which has good generality. In [13, 15, 16, 20, 22], the corresponding controlling functions are expressed as follow:

$$\begin{cases} u(t) = (1 - \lambda t)(1 - t)^2, \\ v(t) = (1 - \lambda + \lambda t)t^2, \end{cases} \tag{3.1}$$

$$\begin{cases} u(t) = (1 - t)^3 + 3\lambda t(1 - t)^2, \\ v(t) = 3\mu t^2(1 - t) + t^3, \end{cases} \tag{3.2}$$

$$\begin{cases} u(t) = (1 - \sin\frac{\pi}{2}t)(1 - \lambda \sin\frac{\pi}{2}t), \\ v(t) = (1 - \cos\frac{\pi}{2}t)(1 - \lambda \cos\frac{\pi}{2}t), \end{cases} \tag{3.3}$$

$$\begin{cases} u(t) = (1 - \sin\frac{\pi}{2}t)(1 - \sin\frac{\pi}{2}t + 2\cos\frac{\pi}{2}t), \\ v(t) = (1 - \cos\frac{\pi}{2}t)(1 - \cos\frac{\pi}{2}t + 2\sin\frac{\pi}{2}t), \end{cases} \tag{3.4}$$

$$\begin{cases} u(t) = [cosh(ln(2 + \sqrt{3})(1 - t)) - 1]^\lambda, \\ v(t) = [cosh(ln(2 + \sqrt{3})t) - 1]^\lambda. \end{cases} \tag{3.5}$$

The properties and applications have been shown respectively in the corresponding references.

To derive new basis efficiently, we provide some simplified construction conditions that $u(t), v(t) \in C^2[0, 1]$ and $t \in (0, 1)$ need to meet

$$\begin{cases} u(t) \geq 0, \quad u'(t) \leq 0, \quad u''(t) > 0, \\ v(t) \geq 0, \quad v'(t) \geq 0, \quad v''(t) > 0, \\ u(0) = 1, \quad u(1) = 0, \quad u'(1) = 0, \\ v(0) = 0, \quad v(1) = 1, \quad v'(0) = 0. \end{cases} \tag{3.6}$$

The definition of the related generating function is shown as follows:

$$\Phi(t) := (u(t), \quad v(t)), \quad t \in [0, 1]. \tag{3.7}$$

First, we will prove that the following space

$$DT_{u,v} = span\{u'(t), \quad v'(t)\} \tag{3.8}$$

is an EC-space on $[0, 1]$. According to Theorem 2.1 of [26], there exists a blossom in the new space $T_{u,v}$, which implies that $T_{u,v}$ is suitable for curve and surface design.

Theorem 1. *Space $DT_{u,v}$ is a two dimensional EC-space on* $[0, 1]$*, where $u(t)$, $v(t)$ satisfy Eq* (3.6).

Proof of Theorem 1. For any $\xi_i \in \mathbb{R}, i = 0, 1, t \in [0, 1]$, we construct a linear equation of $u'(t)$ and $v'(t)$

$$\xi_0 u'(t) + \xi_1 v'(t) = 0. \tag{3.9}$$

Let $t = 0$, from Eq (3.6), it is clear that $\xi_0 = 0$. Similarly, let $t = 1$, we obtain that $\xi_1 = 0$. Therefore, $u'(t)$ and $v'(t)$ are linearly independent, which indicates that the space $DT_{u,v}$ is a two dimensional space on $[0, 1]$. Moreover, we will show $DT_{u,v}$ space is a 2-dimensional ECC-space on $(0, 1)$. When $t \in [a, b] \subseteq (0, 1)$, consider the function

$$h(t) = \left[\frac{v'(t)}{u'(t)}\right]' = \frac{v''(t)u'(t) - v'(t)u''(t)}{(u'(t))^2} < 0. \tag{3.10}$$

When $t \in [a, b]$, two weight functions $w_0(t)$ and $w_1(t)$ are defined as

$$\begin{cases} w_0(t) = -u'(t), \\ w_1(t) = -\lambda h(t), \end{cases} \tag{3.11}$$

where λ is an arbitrary positive real number. Obviously, two weight functions are positive, bounded on $[a, b]$. They also have C^∞ continuity. Define an ECC-space as follows through two weight functions $w_0(t)$ and $w_1(t)$

$$\begin{cases} u_0(t) = w_0(t), \\ u_1(t) = w_0(t) \int_a^t w_1(\tau) d\tau. \end{cases} \tag{3.12}$$

We can prove that both functions $u_i(t)$ $(i = 0, 1)$ can be expressed by $u'(t)$ and $v'(t)$, which shows that $DT_{u,v}$ space is an ECC-space on $[a, b]$. Since $[a, b]$ is an arbitrary subinterval of $(0, 1)$, we come to the conclusion that the space $DT_{u,v}$ is an ECC-space on $(0, 1)$.

Finally, we will show $DT_{u,v}$ space is also an EC-space on $[0, 1]$. We simply need to demonstrate that any nonzero element of the space $DT_{u,v}$ has at most one zero (regardless of multiplicity) on $[0, 1]$. When $t \in [0, 1]$, consider

$$F(t) = C_0 u'(t) + C_1 v'(t), \tag{3.13}$$

where $C_0 \neq 0$ or $C_1 \neq 0$. We have already proved the space $DT_{u,v}$ is an ECC-space on $(0, 1)$, so $F(t)$ has at most one zero on $(0, 1)$. Assuming that $F(0) = 0$, we obtain that $C_0 = 0$ and then, the derivative of $F(t)$ is

$$F'(t) = C_1 v''(t). \tag{3.14}$$

Thus, $F'(t) > 0$, which suggests $F(t)$ is strictly monotonous on [0,1]. We draw the conclusion that there is no zero of $F(t)$ on (0,1). Similarly, by analyzing the case that $F(1) = 0$, we can also obtain that there is at most one zero on $[0, 1]$. As discussed, the space $DT_{u,v}$ is an EC-space on $[0, 1]$. □

According to Theorem 4.1 of [26], we obtain that there is a kind of normalized Bernstein basis on $[0, 1]$ in space $T_{u,v}$. In the next theorem, we give the expression of Chebyshev-Bézier points of the generating function $\Phi(t)$ defined in Eq (3.7) and three generalized quadratic Bernstein-like functions $B_i := B_i^{(0,1)}$ of the space $T_{u,v}$.

Theorem 2. *The three Chebyshev-Bézier points $P_i(i = 0, 1, 2)$ of the generating function $\Phi(t)$ defined in Eq* (3.7) *are given by*

$$P_0 = (1, 0), \quad P_1 = (0, 0), \quad P_2 = (0, 1). \tag{3.15}$$

And generalized quadratic Bernstein-like functions $B_i := B_i^{(0,1)}(i = 0, 1, 2)$ of the space $T_{u,v}$ are given by

$$\begin{cases} B_0(t) = u(t), \\ B_1(t) = 1 - u(t) - v(t), \\ B_2(t) = v(t). \end{cases} \tag{3.16}$$

Proof of Theorem 2. Having given the generating function $\Phi(t)$ in Eq (3.7), it is obvious that

$$\begin{aligned} &\Phi(0) = (1, 0), && \Phi(1) = (0, 1), \\ &\Phi'(0) = (u'(0), 0), && \Phi'(1) = (0, v'(1)). \end{aligned} \tag{3.17}$$

Thus, we obtain

$$\begin{aligned} P_0 = \Phi(0) = (1, 0), \quad P_2 = \Phi(1) = (0, 1), \\ \{P_1\} = \mathrm{Osc}_1\Phi(0) \cap \mathrm{Osc}_2\Phi(1) = (0, 0). \end{aligned} \tag{3.18}$$

When $t \in [0, 1]$, from $\Phi(t) = \sum_{i=0}^{2} B_i(t)P_i$ where $\sum_{i=0}^{2} B_i(t) = 1$, the expressions of the generalized quadratic Bernstein-like functions $B_i(t)$ $(i = 0, 1, 2)$ is easily deduced. □

Remark 3. *By observing the generalized quadratic Bernstein-like functions $B_i(t)$ $(i = 0, 1, 2)$ given in Eq* (3.16)*, it is clear that these basis functions are nonnegative, linearly independent and normalized. In addition, $B_0(1) = 0$ and $B_2(0) = 0$. Thus, according to Theorem 3.11 of [26], the system $(B_0(t), B_1(t), B_2(t))$ is the normalized Bernstein-like basis of the space span $T_{u,v}$. This means that the generalized quadratic Bernstein-like functions are totally positive and have optimal shape preserving properties, such as variation diminishing and monotonicity preserving. More details are shown in references [35–39]. The curve never crosses a hyperplane more often than its control polygon does, because the basis functions have variation diminishing property. Monotonicity preserving means that the monotonicity of the curve is the same as that of monotone control points, and the length of the generated parametric curves is bounded above by the length of their control polygon. If the control polygon is planar and convex, so is the curve.*

There are many controlling functions satisfying Eq (3.6). In the following discussion, we verify three specific examples and then show some figures corresponding to them. To state easily, the generalized quadratic Bernstein-like functions are denoted by $B_i(t; u(t), v(t)), i = 0, 1, 2$, $B_i(t; u(t))$, $i = 0, 1$ and $B_i(t; v(t)), i = 1, 2$.

Example 1. *Consider rational functions having parameters λ and μ. Given controlling functions*

$$\begin{cases} u(t) = (1 - \lambda t)(1 - t)^2, \\ v(t) = (1 - \mu + \mu t)t^2, \end{cases} \tag{3.19}$$

where $-1/2 \leq \lambda, \mu \leq 1$, *we will verify that the controlling functions of Eq* (3.19) *meet Eq* (3.6) *mentioned above. Through substitution and derivation, we have*

$$\begin{cases} u(0) = 1, \quad u(1) = 0, \\ u'(t) = (-\lambda + 3\lambda t - 2)(1 - t) \leq 0, \\ u''(t) = \lambda(-6t + 4) + 2 > 0, \\ v(0) = 0, \quad v(1) = 1, \\ v'(t) = t(3\mu t - 2\mu + 2) \geq 0, \\ v''(t) = \mu(6t - 2) + 2 > 0. \end{cases} \tag{3.20}$$

The generalized quadratic Bernstein-like functions are different when parameters λ *and* μ *are given different values, as shown in Figure 1.*

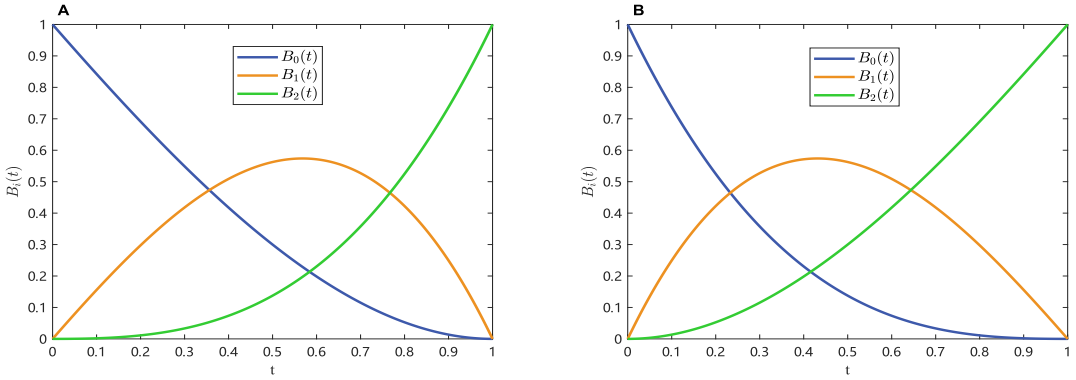

Figure 1. Generalized quadratic Bernstein-like functions given in Eq (3.19); (A) $\lambda = -0.4$, $\mu = 0.9$; (B) $\lambda = 0.9$, $\mu = -0.4$.

Example 2. *Consider trigonometric controlling functions having one parameter* λ. *Given controlling functions*

$$\begin{cases} u(t) = (1 - sin\frac{\pi}{2}t)(1 - \lambda sin\frac{\pi}{2}t), \\ v(t) = (1 - cos\frac{\pi}{2}t)(1 - \lambda cos\frac{\pi}{2}t), \end{cases} \tag{3.21}$$

where $0 \leq \lambda \leq 1$, *we verify that the controlling functions meet Eq* (3.6) *mentioned above. Obviously,*

$$\begin{cases} u(0) = 1, \quad u(1) = 0, \\ u'(t) = \frac{\pi}{2}cos\frac{\pi}{2}t(\lambda(2sin\frac{\pi}{2}t - 1) - 1) \leq 0, \end{cases} \tag{3.22}$$

Then we only need to prove the second derivative of $u(t)$,

$$u''(t) = (\lambda + 1)\frac{\pi^2}{4}sin\frac{\pi}{2}t + \lambda\frac{\pi^2}{2}cos\pi t \tag{3.23}$$

is positive when $t \in (0, 1)$. *As for function defined as*

$$f(x, \lambda) = \pi^2(-\lambda x^2 + \frac{\lambda + 1}{4}x + \frac{\lambda}{2}), \tag{3.24}$$

according to the properties of quadratic polynomial with one variable, we obtain

$$\min_{(0,1)} f(x,\lambda) > min\{f(0,\lambda) = \frac{\pi^2\lambda}{2} \geq 0, f(1,\lambda) = \frac{\pi^2(1-\lambda)}{4} \geq 0\}, \tag{3.25}$$

which implies that u"(t)>0, when $t \in [0,1]$. *Thus,* $u(t)$ *satisfies Eq* (3.6). *Similarly, we can prove that* $v(t)$ *also satisfies Eq* (3.6).

The figures of the accompanying generalized quadratic Bernstein-like functions where λ *is given different values are shown in Figure 2.*

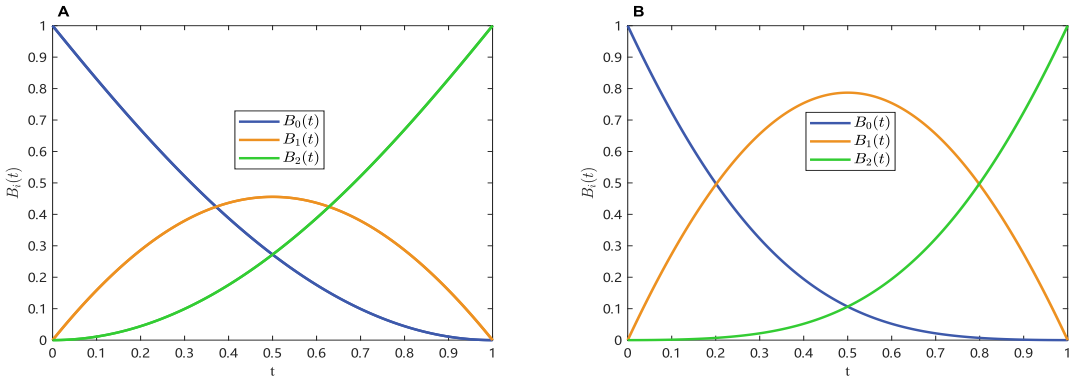

Figure 2. Generalized quadratic Bernstein-like functions given in Eq (3.21); (A) $\lambda = 0.1$; (B) $\lambda = 0.9$.

Example 3. *Consider hyperbolic controlling functions having one exponential parameter* λ. *Given controlling functions*

$$\begin{cases} u(t) = [cosh\, c(1-t) - 1]^{\lambda}, \\ v(t) = (cosh\, ct - 1)^{\lambda}, \end{cases} \tag{3.26}$$

where $c = ln(2 + \sqrt{3}), 1 \leq \lambda \leq 2$, *we verify that these controlling functions also satisfy Eq* (3.6).

Obviously,

$$\begin{cases} u(0) = 1, \quad u(1) = 0, \quad u(t) \geq 0, \\ u'(t) = -c\lambda[cosh\, c(1-t) - 1]^{\lambda-1} sinh\, c(1-t) \leq 0. \end{cases} \tag{3.27}$$

Thus, we only need to prove the second derivative of $u(t)$,

$$u''(t) = c^2\lambda[cosh\, c(1-t) - 1]^{\lambda-2}[(\lambda-1)sinh^2 c(1-t) + (cosh\, c(1-t) - 1)cosh\, c(1-t)] \tag{3.28}$$

is positive for any $t \in (0,1)$. *For cosh c(1-t)>1 and 0<t<1, we know that u''(t)>0. So u(t) satisfies Eq* (3.6). *We can check* $v(t)$ *in the similar way.*

The figures of the accompanying generalized quadratic Bernstein-like functions where λ *is given different values are shown in Figure 3.*

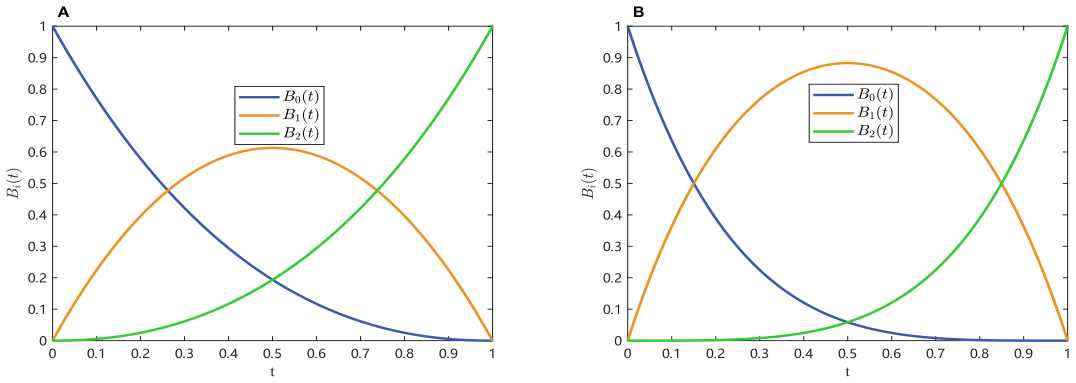

Figure 3. Generalized quadratic Bernstein-like basis functions given in Eq (3.26); (A) λ=1.1; (B) $\lambda = 1.9$.

3.2. New generalized quadratic Bézier curve

Definition 4. *Given control points Q_i $(i = 0, 1, 2)$ in $\mathbb{R}^2$or $\mathbb{R}^3$, $u(t), v(t)$ meeting Eq* (3.6)*, the generalized quadratic Bézier curve with controlling functions $u(t)$ and $v(t)$ is then defined by*

$$Q(t; u(t), v(t)) = \sum_{i=0}^{2} B_i(t; u(t), v(t))Q_i, \quad t \in [0, 1]. \tag{3.29}$$

In [39], Bernstein-Bézier methods are introduced in detail. From the normalization, total positivity and nonnegativity of the new generalized quadratic Bernstein-like functions, which is defined in Eq (3.16), we deduce the corresponding generalized quadratic Bézier curve defined in Eq (3.29) possesses the properties of affine invariance, variation diminishing and convex hull. For curve and surface modeling, these properties count for a great deal. Moreover, through simple calculation, we get the values of the generalized quadratic Bézier curve and its derivative function at 0,1, as shown below:

$$\begin{cases} Q(0; u(t), v(t)) = Q_0, \\ Q(1; u(t), v(t)) = Q_2, \\ Q'(0; u(t), v(t)) = -u'(0)(Q_1 - Q_0), \\ Q'(1; u(t), v(t)) = v'(1)(Q_2 - Q_1). \end{cases} \tag{3.30}$$

The result implies that when $u(t)$ and $v(t)$ meeting Eq (3.6), generalized quadratic Bézier curve is interpolated at the end points. Besides, the corresponding tangents of the curve at Q_0 and Q_2 are exactly Q_0Q_1 and Q_1Q_2. As discussed above, the generalized quadratic Bézier curve proposed in this paper possesses some properties closely similar to quadratic Bézier curve.

Corner cutting algorithms are general treatment of the problem of converting a curve expressed in a B-spline expansion into its Bézier form. It is constructed using convex combinations. Figure 4 shows how corner cutting algorithms are applied to compute the quadratic Bézier curve.

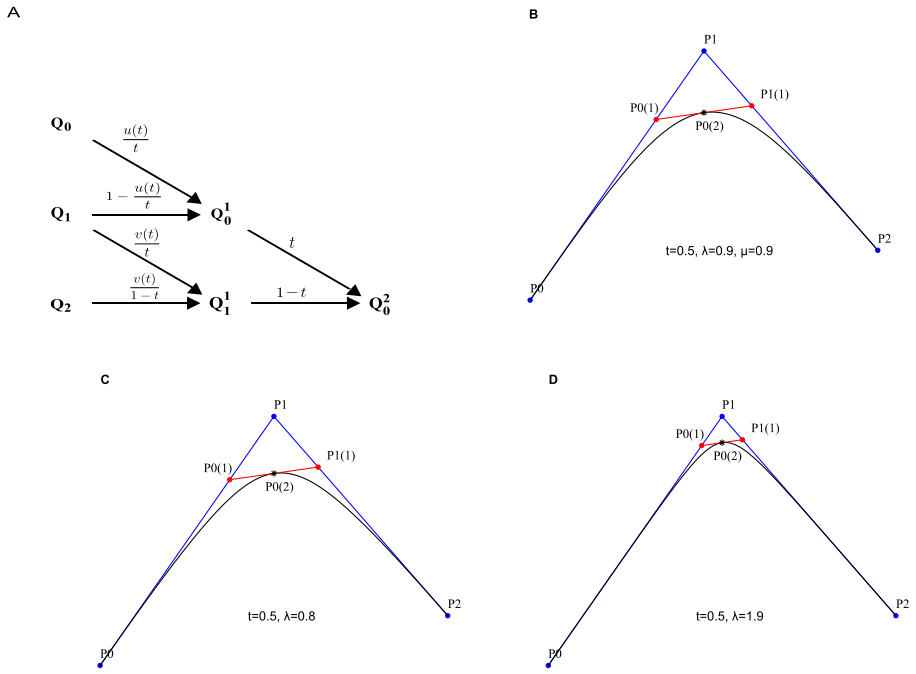

Figure 4. Corner cutting algorithms for constructing the quadratic Bézier curve; (A) The structure of corner cutting algorithms; (B) $u(t)$ and $v(t)$ are given in Eq (3.19) with $t = 0.5$, $\lambda = 0.9$, $\mu = 0.9$; (C) $u(t)$ and $v(t)$ are given in Eq (3.21) with $t = 0.5$, $\lambda = 0.8$; (D) $u(t)$ and $v(t)$ are given in Eq (3.26) with $t = 0.5$, $\lambda = 1.9$.

To develop a similar algorithm and apply to the generalized quadratic Bézier curve, we rewrite the curve in Eq (3.29) as the matrix product form as follows:

$$Q(t;u(t),v(t)) = \begin{pmatrix} t & 1-t \end{pmatrix} \times \begin{pmatrix} \dfrac{u(t)}{t} & 1-\dfrac{u(t)}{t} & 0 \\ 0 & 1-\dfrac{v(t)}{1-t} & \dfrac{v(t)}{1-t} \end{pmatrix} \times \begin{pmatrix} Q_0 \\ Q_1 \\ Q_2 \end{pmatrix}. \tag{3.31}$$

Now it is easy to derive corner cutting algorithms for constructing the generalized quadratic Bernstein-Bézier curve, which is presented in more detail in [36]. In [38], shape preserving approximation is considered when handling the approximation of the control polygon. With reference to these approximate methods introduced in [38], the construction of corner cutting algorithms and some applications of the three cases are given in Figure 4.

Furthermore, when $t \in [0, 1]$, we rewrite Eq (3.29) as

$$Q(t;u(t),v(t)) = Q_1 + B_0(t;u(t))(Q_0 - Q_1) + B_2(t;v(t))(Q_2 - Q_1). \tag{3.32}$$

From Eq (3.32), we notice that $u(t)$ and $v(t)$ only have effects on the curve at its edge $Q_0 - Q_1$ and $Q_2 - Q_1$ respectively. In addition, for any fixed $t \in (0, 1)$, $B_0(t;u(t))$ increases with the increase of $u(t)$. This means that as $u(t)$ increases, the curve will follow edge $Q_0 - Q_1$ in the same direction. On the contrary, when $u(t)$ decreases, the curve moves in the opposite direction to the edge $Q_0 - Q_1$.

The influence of controlling function $v(t)$ on the edge $Q_2 - Q_1$ can be analyzed similarly. Therefore, the controlling functions $u(t)$ and $v(t)$ can be considered as local tension parameters. Their effects on the generalized quadratic Bézier curve are shown in Figure 5, where we change $u(t)$ and $v(t)$ through assigning different values to parameters λ and μ.

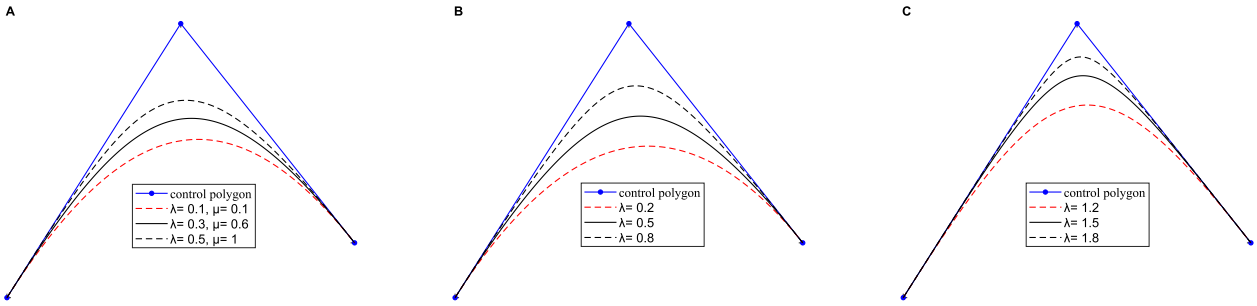

Figure 5. Effects of controlling functions on the generalized quadratic Bézier curve; (A) $u(t)$ and $v(t)$ are given in Eq (3.19); (B) $u(t)$ and $v(t)$ are given in Eq (3.21); (C) $u(t)$ and $v(t)$ are given in Eq (3.26).

4. New generalized quadratic B-splines having controlling functions

Similar to the construction of quadratic B-splines which is based on quadratic Bernstein functions, here we construct generalized quadratic B-splines based on generalized quadratic Bernstein-like functions provided in Eq (3.16).

4.1. New generalized quadratic B-splines

Given knots $u_0 < u_1 < \ldots < u_{n+3}$, a knot vector is denoted by $U = (u_0, u_1, \ldots, u_{n+3})$. Let $h_j = u_{j+1} - u_j$, and $t_j(u) = \left(u - u_j\right)\Big/h_j$, $j = 0, 1, \ldots, n+2$. When $u_i(t), v_i(t)$ $(i = 0, 1, \ldots, n)$ satisfy Eq (3.6), the new generalized quadratic B-splines are constructed as

$$R_i(u) = \begin{cases} R_{i,0}(t_i) = c_i B_2(t_i), & u \in [u_i, u_{i+1}), \\ R_{i,1}(t_{i+1}) = \sum_{j=0}^{2} b_{i+1,j} B_j(t_{i+1}), & u \in [u_{i+1}, u_{i+2}), \\ R_{i,2}(t_{i+2}) = a_{i+2} B_0(t_{i+2}), & u \in [u_{i+2}, u_{i+3}). \\ 0, & u \notin [u_i, u_{i+3}), \end{cases} \tag{4.1}$$

where $B_j(t_i)$ $(i = 0, 1, \ldots, n,\ j = 0, 1, 2)$ are the generalized quadratic Bernstein-like functions provided in Eq (3.16). Consider the properties of C^1 continuity at each knot and normalization on $[u_2, u_{n+1}]$. We know that if a function is C^1-continuous, its first derivative is C^0-continuous at each knot. The C^1 continuity of $R_i(u)$ at u_i is obvious. When $R_i(u)$ is C^1-continuous at u_{i+1}, we obtain

$$\begin{cases} R_i(u_{i+1}^-) &= c_i = R_i(u_{i+1}^+) = b_{i+1,0}, \\ R_i'(u_{i+1}^-) &= \frac{1}{h_i} c_i v_i'(1) = R_i'(u_{i+1}^+) = \frac{1}{h_{i+1}} \left(b_{i+1,0} - b_{i+1,1}\right) u_{i+1}'(0). \end{cases} \tag{4.2}$$

Consider further simplification, we obtain

$$\begin{cases} b_{i+1,0} = c_i, \\ b_{i+1,1} = \dfrac{u_{i+1}^{'}(0)h_{i+1} - v_i^{'}(1)h_{i+1}}{u_{i+1}^{'}(0)h_{i+1}} c_i. \end{cases} \tag{4.3}$$

When $R_i(u)$ is C^1-continuous at u_{i+2}, we obtain

$$\begin{cases} R_i(u_{i+2}^{-}) = b_{i+1,2} = R_i(u_{i+2}^{+}) = a_{i+2}, \\ R_i^{'}(u_{i+2}^{-}) = \frac{1}{h_{i+1}} \left(b_{i+1,2} - b_{i+1,1}\right) v_{i+1}^{'}(1) = R_i^{'}(u_{i+2}^{+}) = \frac{1}{h_{i+2}} a_{i+2} u_{i+2}^{'}(0). \end{cases} \tag{4.4}$$

Consider further simplification, we obtain

$$\begin{cases} b_{i+1,2} = a_{i+2}, \\ b_{i+1,1} = \dfrac{v_{i+1}^{'}(1)h_{i+2} - u_{i+2}^{'}(0)h_{i+1}}{v_{i+1}^{'}(1)h_{i+2}} a_{i+2}. \end{cases} \tag{4.5}$$

Alternatively, we can summarize the calculation results as follows:

$$\begin{cases} b_{i,0} = c_{i-1}, \qquad b_{i,1} = \dfrac{u_i^{'}(0)h_{i-1} - v_{i-1}^{'}(1)h_i}{u_i^{'}(0)h_{i-1}} c_{i-1}, \\ b_{i,2} = a_{i+1}, \qquad b_{i,1} = \dfrac{v_i^{'}(1)h_{i+1} - u_{i+1}^{'}(0)h_i}{v_i^{'}(1)h_{i+1}} a_{i+1}. \end{cases} \tag{4.6}$$

In order to have normalization on $[u_2, u_{n+1}]$, the generalized quadratic B-splines given in Eq (4.1) need to satisfy the equation below

$$\sum_{j=0}^{n} R_j(u) = \sum_{j=i-2}^{i} R_j(u) = \sum_{j=0}^{2} R_{i-j,j}(t_i) = 1. \tag{4.7}$$

For $u \in [u_i, u_{i+1})$, we obtain

$$\sum_{j=0}^{2} R_{i-j,j}(t_i) = R_{i-2,2}(t_i) + R_{i-1,1}(t_i) + R_{i,0}(t_i) = (a_i + b_{i,0})B_0(t_i) + b_{i,1}B_1(t_i) + (b_{i,2} + c_i)B_2(t_i). \tag{4.8}$$

Thus, when $t \in [0, 1]$, from $\sum_{i=0}^{2} B_i(t) = 1$, we can write the equation system of $a_i, b_{i,j}, c_i$ (where $i = 0, 1, \ldots, n$, $j = 0, 1, 2$) as follows:

$$\begin{cases} a_i + b_{i,0} = 1, \\ b_{i,1} = 1, \\ b_{i,2} + c_i = 1. \end{cases} \tag{4.9}$$

Solving the system of equations, we obtain

$$\frac{u_{i+1}^{'}(0)h_i - v_i^{'}(1)h_{i+1}}{u_i^{'}(0)h_{i+1}} c_i = 1. \tag{4.10}$$

To summarize, when the generalized quadratic Bernstein-like functions are C^1-continuous at each knot and have normalization on $[u_2, u_{n+1}]$, the equations of the coefficients are stated as follows:

$$\begin{cases} b_{i+1,2} = a_{i+2} = \dfrac{v'_{i+1}(1)h_{i+2}}{v'_{i+1}(1)h_{i+2} - u'_{i+2}(0)h_{i+1}}, \\ b_{i+1,1} = 1, \\ b_{i+1,0} = c_i = \dfrac{u'_{i+1}(0)h_i}{u'_{i+1}(0)h_i - v'_i(1)h_{i+1}}. \end{cases} \tag{4.11}$$

Definition 5. *With a knot vector U, when $u_i(t), v_i(t)$ meet Eq* (3.6) *and the coefficients $a_i, b_{i,j}, c_i$ meet the above equations, the expressions given in Eq* (4.1) *are defined as the associated generalized quadratic B-splines.*

Figure 6 shows three images of generalized quadratic B-splines when parameters λ and μ are given different values. Here $u(t)$ and $v(t)$ are given in Eqs (3.19), (3.21) and (3.26).

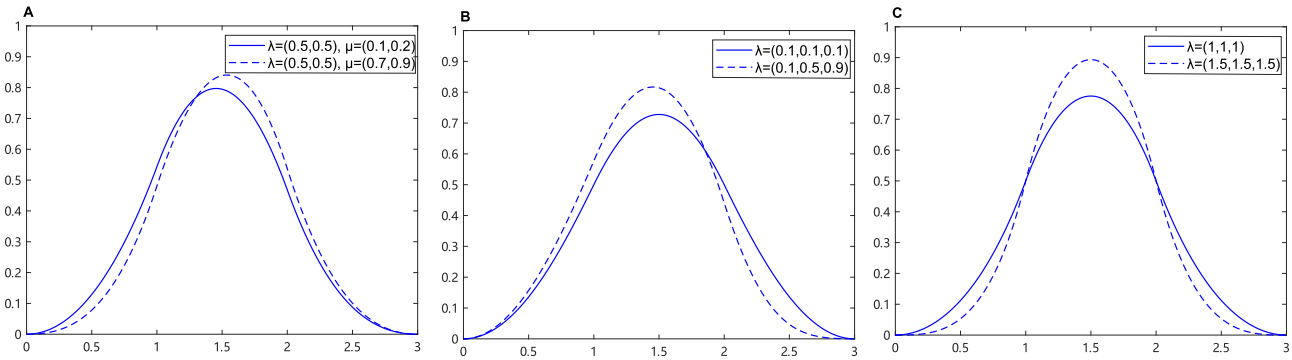

Figure 6. Generalized quadratic B-splines; (A) $u_i(t)$ and $v_i(t)$ are given in Eq (3.19) with $\lambda = (0.5, 0.5)$, $\mu = (0.1, 0.2)$ and $\lambda = (0.5, 0.5)$, $\mu = (0.7, 0.9)$; (B) $u_i(t)$ and $v_i(t)$ are given in Eq (3.21) with $\lambda = (0.1, 0.1, 0.1)$ and $\lambda = (0.1, 0.5, 0.9)$; (C) $u_i(t)$ and $v_i(t)$ are given in Eq (3.26) with $\lambda = (1, 1, 1)$ and $\lambda = (1.5, 1.5, 1.5)$.

Remark 4. *The generalized quadratic B-splines are defined in space* $S := \{s \in C^1[u_0, u_{n+3}]$ *s.t.* $s\big|_{[u_i,u_{i+1}]} \in T_{u,v}\}$, *where $u_i(t), v_i(t)$ satisfy the conditions given in Eq* (3.6), $t_i(u) = (u - u_i)/h_i, i = 0, 1, \ldots, n + 2$.

Remark 5. *Since the coefficients of the B-splines given in Eq* (4.1) *are positive, the generalized quadratic B-splines are also positive. Furthermore, with the property of nonnegativity of the generalized quadratic Bernstein-like functions, the corresponding corner cutting algorithm is stable. Thus, we can form the convex combination and guarantee overall stability. Instability only occurs if we calculate quadratic functions.*

By simple calculation, we can give the expression of the lemma as follows. It is especially efficient for the proofs of normalization and continuity of the generalized quadratic B-splines.

Lemma 1. *For any positive integers i, we have*

$$\begin{cases} b_{i,0} + a_i = 1,\ b_{i,1} = 1, \\ b_{i,2} + c_i = 1, \\ b_{i,0} = c_{i-1}, \\ b_{i,1} = \dfrac{u_i^{'}(0)h_{i-1} - v_{i-1}^{'}(1)h_i}{u_i^{'}(0)h_{i-1}} c_{i-1} = \dfrac{v_i^{'}(1)h_{i+1} - u_{i+1}^{'}(0)h_i}{v_i^{'}(1)h_{i+1}} a_{i+1}, \\ b_{i,2} = a_i. \end{cases} \tag{4.12}$$

4.2. Properties of the new generalized quadratic B-splines

Herein, we will verify the new generalized quadratic B-splines given in Eq (4.1) that have some important properties for curve design and surface construction, which suggest that the splines are normalized (Proposition 1), nonnegative (Proposition 2), linearly independent (Theorem 3), totally positive (Theorem 4) , C^1-continuous (Theorem 5) , C^2-continuous under some certain conditions (Theorem 6), C^3-continuous under some certain conditions (Theorem 7), C^n-continuous under some certain conditions (Theorem 8) and in the case of multiple knots (Theorem 9).

Proposition 1. *For any $u \in [u_2, u_{n+1}]$, we obtain that $\sum_{i=0}^{n} R_i(u) = 1$.*

Proof of Proposition 1. For $u \in [u_i, u_{i+1}), i = 2, 3, \ldots, n$, it is obvious to verify that for $j \neq i-2, i-1, i$, $R_j(u) = 0$. Notice that

$$\begin{cases} R_{i-2}(u) = a_i B_0(t_i), \\ R_{i-1}(u) = \sum\limits_{j=0}^{2} b_{i,j} B_j(t_i), \\ R_i(u) = c_i B_2(t_i), \end{cases} \tag{4.13}$$

by applying Lemma 1, we obtain

$$\sum_{i=0}^{n} R_i(u) = a_i B_0(t_i) + \sum_{j=0}^{2} b_{i,j} B_j(t_i) + c_i B_2(t_i) = \sum_{j=0}^{2} B_j(t_i) = 1. \tag{4.14}$$

According to the equations above, the new generalized quadratic B-splines have normalization. □

Proposition 2. *For $u_i < u < u_{i+3}$, functions $u_i(t), v_i(t)$ satisfying Eq* (3.6)*, $R_i(u) > 0$.*

Proof of Proposition 2. For any $i \in \mathbb{Z}^+$, $j = 0, 1, 2$, when $u_i(t), v_i(t)$ meet Eq (3.6), we obtain that a_i, $b_{i,j}$, c_i>0. Therefore, from the property of positivity of the generalized quadratic Bernstein-like functions $B_j(t_i)$, $R_i(u) > 0$ on (u_i, u_{i+3}). □

Theorem 3. *For any $i \in \mathbb{Z}^+$, $u_i(t), v_i(t)$ satisfying Eq* (3.6)*, the set $\{R_i(u) | i = 0, 1, \cdots, n\}$ is linearly independent on $[u_2, u_{n+1}]$.*

Proof of Theorem 3. For $\xi_i \in \mathbb{R}$ $(i = 0, 1, \ldots, n)$, functions $u_i(t), v_i(t)$ satisfying Eq (3.6), $u \in [u_2, u_{n+1}]$, let

$$R(u) = \sum_{i=0}^{n} \xi_i R_i(u) = 0. \tag{4.15}$$

With straightforward computation, we obtain

$$R(u_i) = a_i\xi_{i-2} + b_{i,0}\xi_{i-1} = 0, \tag{4.16}$$

$$R'(u_i) = \frac{1}{h_i}\left[a_i u_i^{'}(0)\xi_{i-2} + (b_{i,0} - b_{i,1})\, u_i^{'}(0)\xi_{i-1}\right] = 0, \tag{4.17}$$

where $i = 2, 3, \ldots, n+1$. Thus, the linear system of equations about ξ_{i-2}, ξ_{i-1} are as follows:

$$\begin{cases} a_i\xi_{i-2} + b_{i,0}\xi_{i-1} = 0, \\ a_i u_i^{'}(0)\xi_{i-2} + (b_{i,0} - b_{i,1})\, u_i^{'}(0)\xi_{i-1} = 0. \end{cases} \tag{4.18}$$

Notice that $a_i + b_{i,0} = 1$, to compute the determinant of the coefficient matrix C_i given by the above linear equation system. The specific expression of the determinant is shown as follows:

$$\begin{aligned} |C_i| &= \begin{vmatrix} a_i & b_{i,0} \\ a_i u_i^{'}(0) & (b_{i,0} - b_{i,1}) u_i^{'}(0) \end{vmatrix} \\ &= \begin{vmatrix} a_i & b_{i,1} \\ a_i u_i^{'}(0) & 0 \end{vmatrix} \\ &= -a_i b_{i,1} u_i^{'}(0) \\ &> 0. \end{aligned} \tag{4.19}$$

Thus, we can come to a conclusion that for $i = 2, 3, \ldots, n+1$, $\xi_{i-2} = \xi_{i-1} = 0$, which suggests that the set $\{R_i(u) | i = 0, 1, \cdots, n\}$ is linearly independent on $[u_2, u_{n+1}]$. □

Theorem 4. *For $u \in [u_i, u_{i+1}]$, $u_i(t), v_i(t)$ satisfying Eq (3.6), $i = 2, 3, \ldots, n$, the system $(R_{i-2}(u), R_{i-1}(u), R_i(u))$ is a normalized totally positive basis of the space span $T_{u,v}$.*

Proof of Theorem 4. For $u \in [u_i, u_{i+1}]$, $i = 2, 3, \ldots, n$, functions $u_i(t), v_i(t)$ satisfying Eq (3.6), $t_i(u) = (u - u_i)/h_i$, we can easily verify that

$$(R_{i-2}(u), R_{i-1}(u), R_i(u)) = (B_0(t_i), B_1(t_i), B_2(t_i))\, H_i, \tag{4.20}$$

where

$$H_i = \begin{bmatrix} a_i & b_{i,0} & 0 \\ 0 & b_{i,1} & 0 \\ 0 & b_{i,2} & c_i \end{bmatrix}. \tag{4.21}$$

Since the system $(B_0(t_i), B_1(t_i), B_2(t_i))$ is the normalized B-basis of the space $T_{u,v}$, according to Theorem 4.2 of [38], we can conclude that H_i is a nonsingular stochastic and totally positive matrix. For functions $u_i(t), v_i(t)$ meeting Eq (3.6), $i \in \mathbb{Z}^+$, $j = 0, 1, 2$, it is obvious to verify that a_i, $b_{i,j}$ c_i>0. Moreover, it is easy to obtain that H_i is stochastic from Lemma 1. This shows that Theorem 4 is true. □

Theorem 5. *With a non-uniform knot vector, the generalized quadratic B-splines $R_i(u)$ with $u_i(t), v_i(t)$ meeting Eq (3.6) is C^1-continuous at each knot.*

Proof of Theorem 5. We consider the continuity at u_{i+1} first. For functions $u_i(t), v_i(t)$ satisfying Eq (3.6), we obtain

$$\begin{aligned} &R_i(u_{i+1}^-) = c_i, \qquad R_i(u_{i+1}^+) = b_{i+1,0}, \\ &R_i'(u_{i+1}^-) = \frac{c_i v_i^{'}(1)}{h_i}, \quad R_i'(u_{i+1}^+) = \frac{(b_{i+1,0} - b_{i+1,1})\, u_{i+1}^{'}(0)}{h_{i+1}}. \end{aligned} \tag{4.22}$$

We know that the theorem is true at u_{i+1} from the equations above and Lemma 1. We can similarly analyze the theorem at other knots. □

Theorem 6. *With the property of having C^1 continuity at each knot discussed above, when controlling functions $u_i(t), v_i(t)$ satisfy*

$$\begin{cases} u_i^{''}(1) = 0, \\ v_i^{''}(0) = 0, \\ \dfrac{u_{i+1}^{''}(0)}{u_{i+1}^{'}(0)} h_i = \dfrac{v_i^{''}(1)}{v_i^{'}(1)} h_{i+1}, \end{cases} \tag{4.23}$$

the generalized quadratic B-splines $R_i(u)$ are C^2-continuous at each knot.

Proof of Theorem 6. On the basis of the proof that the generalized quadratic B-splines $R_i(u)$ have C^1 continuity with fixed coefficients $a_i, b_{i,j}, c_i$, we only need to verify the second derivative is continuous in order to have C^2 continuity. Next, we will prove that $R_i(u)$ are C^2-continuous at each knot.

We calculate the second derivative of $R_i(u)$ at u_i, u_{i+1} , u_{i+2} and u_{i+3}, which are

$$\begin{cases} R_i^{''}(u_i) = \dfrac{c_i}{h_i^2} v_i^{''}(0), \\ R_i^{''}(u_{i+1}^-) = \dfrac{1}{h_i^2} c_i v_i^{''}(1), \\ R_i^{''}(u_{i+1}^+) = \dfrac{1}{h_{i+1}^2} (b_{i+1,0} - b_{i+1,1})\, u_{i+1}^{''}(0), \\ R_i^{''}(u_{i+2}^-) = \dfrac{1}{h_{i+1}^2} (b_{i+1,2} - b_{i+1,1})\, v_{i+1}^{''}(1), \\ R_i^{''}(u_{i+2}^+) = \dfrac{1}{h_{i+2}^2} a_{i+2} u_{i+2}^{''}(0), \\ R_i^{''}(u_{i+3}) = \dfrac{a_{i+2}}{h_{i+2}^2} u_{i+2}{}^{''}(1). \end{cases} \tag{4.24}$$

When the controlling functions $u_i(t)$ and $v_i(t)$ meet Eq (4.23), we obtain

$$\begin{cases} R_i^{''}(u_i) = 0, \\ R_i^{''}(u_{i+1}^-) = R_i^{''}(u_{i+1}^+), \\ R_i^{''}(u_{i+2}^-) = R_i^{''}(u_{i+2}^+), \\ R_i^{''}(u_{i+3}) = 0, \end{cases} \tag{4.25}$$

which show that $R_i(u)$ have C^2 continuity at each knot.

These indicate that the generalized quadratic B-splines $R_i(u)$ are C^2-continuous at each knot. □

Example 4. *Given knots $u_0 < u_1 < \cdots < u_{i+3}$, the controlling functions are given as follows:*

$$\begin{cases} u(t) = \left(1 - sin\frac{\pi}{2}t\right)\left(1 - sin\frac{\pi}{2}t + 2cos\frac{\pi}{2}t\right), \\ v(t) = \left(1 - cos\frac{\pi}{2}t\right)\left(1 - cos\frac{\pi}{2}t + 2sin\frac{\pi}{2}t\right). \end{cases} \tag{4.26}$$

We will verify that these controlling functions given in Eq (4.26) *satisfy Eq* (3.6)*. We calculate their derivative where endpoint values are 0 and 1, which are*

$$\begin{cases} u(0) = 1, \quad u(1) = 0, \\ u'(t) = \dfrac{\pi}{2}\left(-2cos\frac{\pi}{2}t - 2sin\frac{\pi}{2}t + sin\pi t - 2cos\pi t\right) \le 0, \\ u''(t) = \dfrac{\pi^2}{4}\left(2sin\frac{\pi}{2}t - 2cos\frac{\pi}{2}t + 2cos\pi t + 4sin\pi t\right) \ge 0, \\ v(0) = 0, \quad v(1) = 1, \\ v'(t) = \dfrac{\pi}{2}\left(2sin\frac{\pi}{2}t + 2cos\frac{\pi}{2}t - sin\pi t - 2cos\pi t\right) \ge 0, \\ v''(t) = \dfrac{\pi^2}{4}\left(2cos\frac{\pi}{2}t - 2sin\frac{\pi}{2}t - 2cos\pi t + 4sin\pi t\right) \ge 0. \end{cases} \tag{4.27}$$

This implies that Example 4 satisfy Eq (3.6)*. Next, we calculate both first and second derivatives of $u(t), v(t)$ where endpoint values are* 0, 1*,*

$$\begin{cases} u'(0) = -2\pi, \quad u''(0) = 0, \\ v'(1) = 2\pi, \quad v''(1) = 0, \end{cases} \tag{4.28}$$

which satisfy Eq (4.23)*. So it can be concluded that the generalized quadratic B-splines having controlling functions given in Eq* (4.26) *are C^2-continuous at each knot.*

Theorem 7. *With the property of C^2 continuity at each knot discussed above, when the controlling functions $u_i(t), v_i(t)$ meet*

$$\begin{cases} u_i^{(3)}(1) = 0, \\ v_i^{(3)}(0) = 0, \\ \dfrac{u_{i+1}^{(3)}(0)}{u_{i+1}^{'}(0)}h_i^2 = \dfrac{v_i^{(3)}(1)}{v_i^{'}(1)}h_{i+1}^2, \end{cases} \tag{4.29}$$

the generalized quadratic B-splines $R_i(u)$ are C^3-continuous at each knot.

Proof of Theorem 7. Based on the proof that the generalized quadratic B-splines $R_i(u)$ are C^2-continuous with fixed coefficients $a_i, b_{i,j}, c_i$, we only need to verify their third derivative is continuous in order to have C^3 continuity. Next, we will prove that $R_i(u)$ are C^3-continuous at each knot.

We calculate the third derivative of $R_i(u)$ at each knot, which are

$$\begin{cases} R_i^{(3)}(u_i) = \dfrac{c_i}{h_i^3} v_i^{(3)}(0), \\ R_i^{(3)}(u_{i+1}^-) = \dfrac{1}{h_i^3} c_i v_i^{(3)}(1), \\ R_i^{(3)}(u_{i+1}^+) = \dfrac{1}{h_{i+1}^3} \left(b_{i+1,0} - b_{i+1,1}\right) u_{i+1}^{(3)}(0), \\ R_i^{(3)}(u_{i+2}^-) = \dfrac{1}{h_{i+1}^3} \left(b_{i+1,2} - b_{i+1,1}\right) v_{i+1}^{(3)}(1), \\ R_i^{(3)}(u_{i+2}^+) = \dfrac{1}{h_{i+2}^3} a_{i+2} u_{i+2}^{(3)}(0), \\ R_i^{(3)}(u_{i+3}) = \dfrac{a_{i+2}}{h_{i+2}^3} u_{i+2}{}^{(3)}(1). \end{cases} \tag{4.30}$$

When the controlling functions $u_i(t)$ and $v_i(t)$ meet Eq (4.29), we obtain

$$\begin{cases} R_i^{(3)}(u_i) = 0, \\ R_i^{(3)}(u_{i+1}^-) = R_i^{(3)}(u_{i+1}^+), \\ R_i^{(3)}(u_{i+2}^-) = R_i^{(3)}(u_{i+2}^+), \\ R_i^{(3)}(u_{i+3}) = 0, \end{cases} \tag{4.31}$$

which show that $R_i(u)$ are C^3-continuous at each knot.

Thus, we can come to a conclusion that the generalized quadratic B-splines $R_i(u)$ are C^3-continuous at each knot. □

Example 5. *Given equidistant knots $u_0 < u_1 < \cdots < u_{i+3}$, the controlling functions are given as follows:*

$$\begin{cases} u(t) = \frac{1}{8}\left(8 - 9sin\frac{\pi}{2}t - sin\frac{3\pi}{2}t\right), \\ v(t) = \frac{1}{8}\left(8 - 9cos\frac{\pi}{2}t + cos\frac{3\pi}{2}t\right). \end{cases} \tag{4.32}$$

We will verify that these controlling functions given in Eq (4.32) *satisfy Eq* (3.6)*. We calculate their derivative where endpoint values are 0 and 1, which are*

$$\begin{cases} u(0) = 1, \quad u(1) = 0, \\ u'(t) = \frac{\pi}{16}\left(-9cos\frac{\pi}{2}t - 3cos\frac{3\pi}{2}t\right) \le 0, \\ u''(t) = \frac{\pi^2}{32}\left(9sin\frac{\pi}{2}t + 9sin\frac{3\pi}{2}t\right) \ge 0, \\ v(0) = 0, \quad v(1) = 1, \\ v'(t) = \frac{\pi}{16}\left(9sin\frac{\pi}{2}t - 3sin\frac{3\pi}{2}t\right) \ge 0, \\ v''(t) = \frac{\pi^2}{32}\left(9cos\frac{\pi}{2}t - 9cos\frac{3\pi}{2}t\right) \ge 0. \end{cases} \tag{4.33}$$

This implies that Example 5 satisfy Eq (3.6)*. Next, we calculate both first and second derivatives of $u(t), v(t)$ at the endpoint value 0 and 1 respectively, we have*

$$\begin{cases} u'(0) = -\frac{3}{4}\pi, \quad u''(0) = 0, \\ v'(1) = \frac{3}{4}\pi, \quad v''(1) = 0, \end{cases} \tag{4.34}$$

which satisfy Eq (4.23)*. So we conclude that the generalized quadratic B-splines with controlling functions provided in Eq* (4.32) *are C^2-continuous at each knot.*

Next, we calculate the third derivative of $u(t), v(t)$ where endpoint values are 0 and 1, which are

$$\begin{cases} u^{(3)}(0) = \frac{9}{16}\pi, \\ v^{(3)}(1) = -\frac{9}{16}\pi. \end{cases} \tag{4.35}$$

For equidistant knots, consider Eqs (4.34) *and* (4.35)*, we find that they satisfy Eq* (4.29)*. So we conclude that the generalized quadratic B-splines having controlling functions $u(t), v(t)$ provided in Eq* (4.32) *have C^3 continuity at each equidistant knot.*

Theorem 8. *For all $n \in \mathbb{Z}^+$, if the controlling functions $u_i(t), v_i(t)$ satisfy*

$$\begin{cases} u_i^{(m)}(1) = 0, \\ v_i^{(m)}(0) = 0, \\ \dfrac{u_{i+1}^{(m)}(0)}{u_{i+1}^{'}(0)} h_i^{m-1} = \dfrac{v_i^{(m)}(1)}{v_i^{'}(1)} h_{i+1}^{m-1}, \end{cases} \tag{4.36}$$

where $m = 1, 2, \cdots, n$, the generalized quadratic B-splines $R_i(u)$ have C^n continuity at each knot.

Proof of Theorem 8. We prove it by mathematical induction. For $n = 1$, the conclusion is established according to Theorem 6. Assuming the theorem holds when $n = k$(for some $k \in \mathbb{Z}^+$), we obtain that the generalized quadratic B-splines $R_i(u)$ have C^k continuity at each knot, and Eq (4.36) holds for $m = 1, 2, \cdots, k$. Thus, for $n = k + 1$, the controlling functions $u_i(t), v_i(t)$ only need to satisfiy Eq (4.36) where $m = k + 1$ to have C^n continuity. Next, we calculate $(k+1)$-th derivative of $R_i(u)$ at each knot, which are

$$\begin{cases} R_i^{(k+1)}(u_i) = \frac{c_i}{h_i^{k+1}} v_i^{(k+1)}(0), \\ R_i^{(k+1)}(u_{i+1}^-) = \frac{1}{h_i^{k+1}} c_i v_i^{(k+1)}(1), \\ R_i^{(k+1)}(u_{i+1}^+) = \frac{1}{h_{i+1}^{k+1}} \left(b_{i+1,0} - b_{i+1,1}\right) u_{i+1}^{(k+1)}(0), \\ R_i^{(k+1)}(u_{i+2}^-) = \frac{1}{h_{i+1}^{k+1}} \left(b_{i+1,2} - b_{i+1,1}\right) v_{i+1}^{(k+1)}(1), \\ R_i^{(k+1)}(u_{i+2}^+) = \frac{1}{h_{i+2}^{k+1}} a_{i+2} u_{i+2}^{(k+1)}(0), \\ R_i^{(k+1)}(u_{i+3}) = \frac{a_{i+2}}{h_{i+2}^{k+1}} {u_{i+2}}^{(k+1)}(1). \end{cases} \tag{4.37}$$

These indicate that the controlling functions $u_i(t)$ and $v_i(t)$ satisfy Eq (4.36) where $m = k + 1$, which are

$$\begin{cases} R_i^{(k+1)}(u_i) = 0, \\ R_i^{(k+1)}(u_{i+1}^-) = R_i^{(k+1)}(u_{i+1}^+), \\ R_i^{(k+1)}(u_{i+2}^-) = R_i^{(k+1)}(u_{i+2}^+), \\ R_i^{(k+1)}(u_{i+3}) = 0. \end{cases} \tag{4.38}$$

These indicate that $R_i(u)$ have C^{k+1} continuity at each knot. Thus, the generalized quadratic B-splines $R_i(u)$ are C^{k+1}-continuous.

Thus, we now know from mathematical induction that the theorem holds for $n \in \mathbb{Z}^+$. □

The above discussion is based on the strictly monotonically increasing sequence of simple knots. Multiple knots will affect the smoothness and numerical stability of the basis functions. In order to construct well-defined generalized quadratic B-splines at multiple knots, we delete the intervals that shrink to zero. Without loss of generality, we study the case where $u_i = u_{i+1}$, here we define

$$R_i(u) = \begin{cases} R_{i,1}(t_{i+1}) = \sum_{j=0}^{2} b_{i+1,j} B_j(t_{i+1}), & u \in [u_{i+1}, u_{i+2}), \\ R_{i,2}(t_{i+2}) = a_{i+2} B_0(t_{i+2}), & u \in [u_{i+2}, u_{i+3}), \\ 0, & u \notin [u_i, u_{i+3}). \end{cases} \tag{4.39}$$

Theorem 9. *Suppose that the basis functions have a knot of multiplicity k (k = 2 or 3) at a parameter value u. Then at this piont the continuity of the basis function is reduced from C^n to C^{n+1-k} (C^{-1} means discontinous).*

Proof of Theorem 9. In the case of $k = 2$, $u_i = u_{i+1}$, $h_i = 0$.

$$b_{i+1,0} = c_i = \frac{u'_{i+1}(0)h_i}{u'_{i+1}(0)h_i - v'_i(1)h_{i+1}} = 0, \tag{4.40}$$

$$b_{i+1,1} = 1. \tag{4.41}$$

By Theorem 8, we obtain $u_{i+1}^{m-1}(0) = 0$, where $m = 1, 2, \cdots, n$. Obviously

$$R_i^{(m-1)}(u_{i+1}^+) = -\frac{1}{h_{i+1}^{m-1}} u_{i+1}^{(m-1)}(0) = 0. \tag{4.42}$$

That is, the continuity of the basis decreases from C^n to C^{n-1}.
Similarly, the case of $k = 3$ can be proved. □

5. New generalized quadratic B-spline curves

Definition 6. *Given a knot vector U and some control points Q_i ($i = 0, 1, \ldots, n$) in $\mathbb{R}^2$ or $\mathbb{R}^3$, for $u_i(t), v_i(t)$ meeting Eq (3.6) and any integers $n \geq 2$, $u \in [u_2, u_{n+1}]$, a new generalized quadratic B-spline curve having two functions $u_i(t), v_i(t)$ is defined by*

$$R(u) = \sum_{i=0}^{n} R_i(u) Q_i, \tag{5.1}$$

It is obvious that for $u \in [u_i, u_{i+1}]$, $i = 2, 3, \ldots, n$, the curve $R(u)$ can be rewritten by the following curve segment

$$R(u) = \sum_{j=i-2}^{i} R_j(u) Q_j = (a_i Q_{i-2} + b_{i,0} Q_{i-1}) B_0(t_i) + b_{i,1} Q_{i-1} B_1(t_i) + (b_{i,2} Q_{i-1} + c_i Q_i) B_2(t_i). \tag{5.2}$$

According to Theorems 1 and 2, the generalized quadratic B-splines are normalized and nonnegative. Thus, the corresponding new generalized quadratic B-spline curve $R(u)$ has affine invariance. When $u \in [u_i, u_{i+1}]$, $R(u)$ lies in the control polygon formed by Q_{i-2}, Q_{i-1}, Q_i. According to Theorem 4, since the generalized quadratic B-splines are totally positive, the accompanying B-spline curve $R(u)$ has variation diminishing. This means $R(u)$ can be used in shape control.

5.1. Relationship between generalized quadratic B-spline curves and controlling functions

According to the previous discussion of properties, by changing different shape parameters of controlling functions, we get the desired shape of the curve. As we increase the values of these parameters, the curves will move near to the control polygon. Next, we demonstrate this relationship in detail with two examples.

Example 6. *Figure 7 shows the closed spline curves in the shape of a fish, which are constructed with $u_i(t)$ and $v_i(t)$ provided in Eq* (3.19) *having distinct controlling parameters. Let all $\lambda_i = 0.1, \mu_i = 0, 2$, we can obtain the first figure. By changing the value of one λ_i based on the first one, we can obtain the second figure. By changing the value of another λ_i based on the second one, we can obtain the third figure. The curvature comb plots in the corresponding rectangles are also shown.*

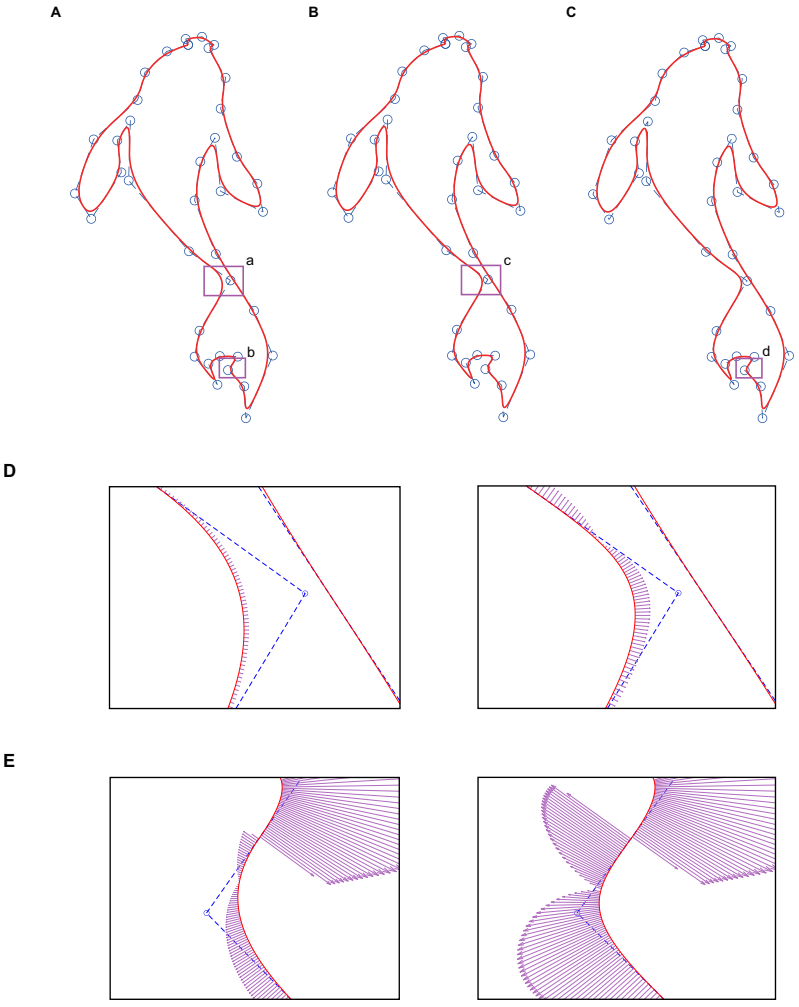

Figure 7. Closed curves with uniform knot vector of the controlling functions with $u_i(t)$ and $v_i(t)$ given in Eq (3.19); (A) All $\lambda_i = 0.1, \mu_i = 0, 2$; (B) Changing the value of one λ_i from 0.1 to 1 based on A; (C) Changing the value of another λ_i from 0.1 to 1 based on B; (D) The curvature comb plots in rectangles a and c; (E) The curvature comb plots in rectangles b and d.

Example 7. *Figure 8 shows the closed spline curves in the shape of a cat, which are constructed with $u_i(t)$ and $v_i(t)$ provided in Eq* (3.21) *having distinct controlling parameters. Let all $\lambda_i = 0.2$, we can obtain the first figure. By changing the value of one λ_i based on the first one, we can obtain the second figure. By changing the value of two other μ_i based on the second one, we can obtain the third figure. The curvature comb plots in the corresponding rectangles are also shown.*

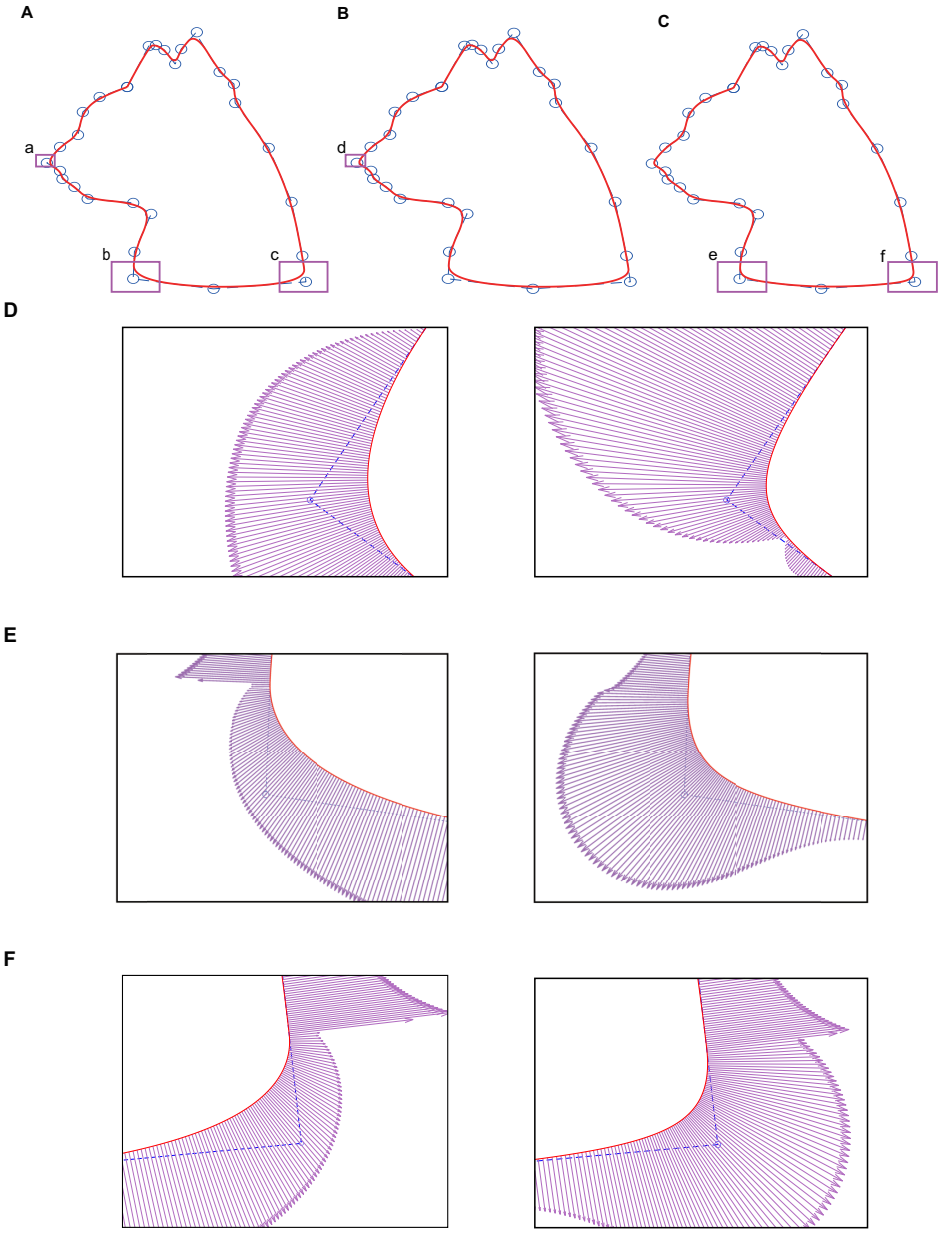

Figure 8. Closed curves with uniform knot vector of the controlling functions with $u_i(t)$ and $v_i(t)$ given in Eq (3.21); (A) All $\lambda_i = 0.2$; (B) Changing the value of one λ_i from 0.2 to 0.5 based on A; (C) Changing the value of two other μ_i from 0.2 to 0.5 based on B; (D) The curvature comb plots in rectangles a and d; (E) The curvature comb plots in rectangles b and e; (F) The curvature comb plots in rectangles c and f.

5.2. Continuity conditions of generalized quadratic B-spline curves

It is hard to construct complex curves under continuity conditions of traditional Bézier curves. While the generalized quadratic B-spline curves have alternative controlling functions, they help us construct complex curves under parametric continuity conditions.

Proposition 3. *With a non-uniform knot vector, the new generalized quadratic B-spline curves $R(u)$ are C^1-continuous. Furthermore, if u_i is a simple knot, for $i = 2, 3, \ldots, n+1$, we obtain*

$$R(u_i) = a_i Q_{i-2} + b_{i,0} Q_{i-1}, \tag{5.3}$$

$$R'(u_i) = \frac{a_i u_i'(0)}{h_i} Q_{i-2} + \frac{(b_{i,0} - b_{i,1})\, u_i'(0)}{h_i} Q_{i-1}. \tag{5.4}$$

Proposition 4. *With a non-uniform knot vector, for all $n \in \mathbb{Z}^+$, if the controlling functions $u_i(t), v_i(t)$ satisfy the conditions given in Theorm 8, the generalized quadratic B-spline curves $R(u)$ are C^n-continuous.*

Example 8. *Figure 9 shows the comparison among the traditional quadratic B-spline curve and the generalized quadratic B-spline curves which are constructed with $u_i(t)$ and $v_i(t)$ given in Eq* (4.26) *and Eq* (4.32). *The traditional quadratic B-spline curve is C^1-continuous. The second one is C^2-continuous, which has been proved in Example 4. The third one is C^3-continuous, which has been proved in Example 5. The curvature comb plots in the corresponding rectangles are also shown.*

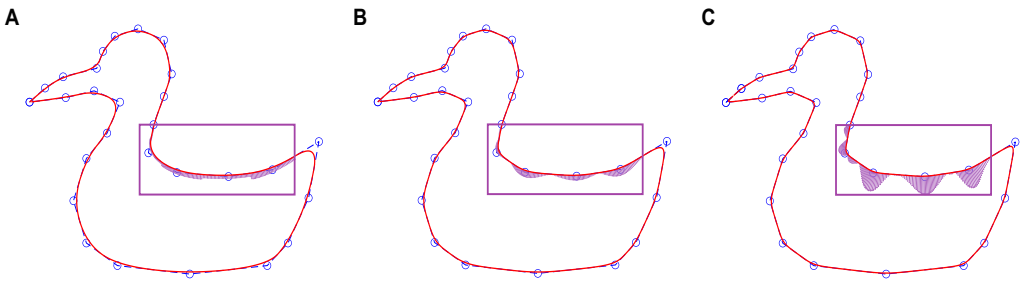

Figure 9. Closed curves with the controlling functions with different continuity; (A) C^1 continuity, traditional quadratic B-splines; (B) C^2 continuity, functions given in Eq (4.26); (C) C^3 continuity, functions given in Eq (4.32).

Example 9. *Figure 10 shows the 3-dimensional open spline curves, which are constructed with $u_i(t)$ and $v_i(t)$ given in Eq* (3.19).

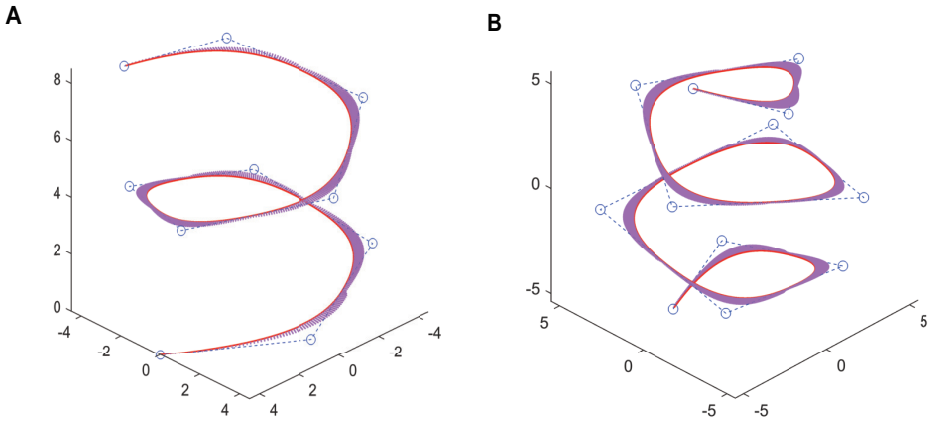

Figure 10. 3-dimensional open spline curves.

6. Disscusion

In this work, we construct generalized quadratic B-splines having controlling functions. It includes rational B-spline and some advanced work. We further explore the conditions for higher-order continuity, which are of practical use in industrial design.

The proposed generalized B-splines have many excellent properties. For example, the controlling functions given in Example 2 can accurately represent ellipses, see [16]. The controlling functions given in Example 3 can accurately represent hyperbolas. Besides, the curve can achieve G^3 smooth splicing at the junctions under certain conditions, see [22]. These cannot be executed by traditional B-spline and its algorithms.

Traditional quadratic B-splines and some quasi quadratic B-splines are C^1 continuous, which cannot meet the needs of many practical applications. Based on C^1 continuity, our generalized B-spline can achieve C^2 continuity, C^3 continuity, or even higher continuity under some conditions we propose.

Traditional B-splines and NURBS can adjust curves locally. However, the effects are limited. The proposed generalized B-splines with controlling functions include many splines with better shape control effects. We give some plots to show the effects of this more flexible and varied shape control. Analogous to NURBS, we can locally modify curves by adjusting the shape parameters in corresponding positions. Therefore, it is achievable to embed the proposed generalized B-splines in CAD systems.

We will continue to explore further applications of these generalized quadratic B-splines having controlling functions and embed such splines in modeling software in the future.

7. Conclusions

We introduced generalized quadratic Bernstein-like functions having controlling functions and analyzed their properties. It includes the basis given in [13–20] as special cases. The controlling functions satisfying specific conditions have wide applications, with three cases presented. The accompanying generalized quadratic Bézeir curves and corner cutting algorithms are provided. Taking the new basis functions as a foundation, we proposed generalized quadratic B-splines. They are

normalized, nonnegative, linearly independent, totally positive and C^1-continuous. These properties are crucial in curve modeling. We further explore the condition that the basis needs to meet for C^2 and C^3 continuity, and extend it to the condition of C^n continuity. It greatly expands the application range of generalized quadratic B-splines. The generalized quadratic B-spline curves and their applications are shown.

Use of AI tools declaration

The authors declare they have not used Artificial Intelligence (AI) tools in the creation of this article.

Acknowledgements

The research is supported by the National Natural Science Foundation of China (No. 61802129) and the Fundamental Research Funds for the Central Universities (No. 2022ZYGXZR064).

Conflict of interest

The authors declare no conflict of interest.

References

1. R. Wang, C. Li, C. Zhu, *Computational geometry tutorial (Chinese)*, Beijing: Science Press, 2008.
2. X. Zhu, *Free-form curve and surface modeling technology (Chinese)*, Beijing: Science Press, 2000.
3. R. Wang, *Numerical rational approximation (Chinese)*, Shanghai: Shanghai Scientific and Technical Publishers, 1980.
4. C. de Boor, On calculating with B-splines, *J. Approx. Theory*, **6** (1972), 50–62. https://doi.org/10.1016/0021-9045(72)90080-9
5. K. Versprille, Computer-aided design applications of the rational b-spline approximation form, Ph. D Thesis, Syracuse University, 1975.
6. L. Ramshaw, *Blossoming: a connect-the-dots approach to splines*, Palo Alto: Digital Equipment Corporation, 1987.
7. M. Mazure, P. Laurent, Piecewise smooth spaces in duality: application to blossoming, *J. Approx. Theory*, **98** (1999), 316–353. https://doi.org/10.1006/jath.1998.3306
8. M. Mazure, Quasi-chebyshev splines with connection matrices: application to variable degree polynomial splines, *Comput. Aided Geom. D.*, **18** (2001), 287–298. https://doi.org/10.1016/s0167-8396(01)00031-0
9. M. Mazure, Blossoms and optimal bases, *Adv. Comput. Math.*, **20** (2004), 177–203. https://doi.org/10.1023/A:1025855123163
10. P. Costantini, T. Lyche, C. Manni, On a class of weak Tchebycheff systems, *Numer. Math.*, **101** (2005), 333–354. https://doi.org/10.1007/s00211-005-0613-6

11. M. Mazure, On dimension elevation in quasi extended Chebyshev spaces, *Numer. Math.*, **109** (2008), 459–475. https://doi.org/10.1007/s00211-007-0133-7
12. P. Costantini, F. Pelosi, M. Sampoli, New spline spaces with generalized tension properties, *BIT Numer. Math.*, **48** (2008), 665–688. https://doi.org/10.1007/s10543-008-0195-7
13. X. Han, S. Liu, Extension of a quadratic Bézier curve (Chinese), *Journal of Central South University (Science and Technology)*, **34** (2003), 214–217.
14. J. Xie, S. Hong, Quadratic B-spline curve with shape parameters (Chinese), *Computer Aided Engineering*, **15** (2006), 15–19.
15. L. Yan, T. Liang, The quadratic Bézier curves that shape can adjust (Chinese), *Journal of East China University of Technology (Natural Science)*, **31** (2008), 93–97.
16. X. Han, Quadratic trigonometric polynomial curves with a shape parameter, *Comput. Aided Geom. D.*, **19** (2002), 503–512. https://doi.org/10.1016/s0167-8396(02)00126-7
17. X. Wu, Research on the theories and methods of geometric modeling based on the curves and surfaces with shape parameter, Ph. D Thesis, Central South University, 2008.
18. X. Han, Quadratic trigonometric polynomial curves concerning local control, *Appl. Numer. Math.*, **56** (2006), 105–115. https://doi.org/10.1016/j.apnum.2005.02.013
19. X. Han, Piecewise quadratic trigonometric polynomial curves, *Math. Comput.*, **72** (2003), 1369–1377. https://doi.org/10.1090/s0025-5718-03-01530-8
20. X. Han, C^2 quadratic trigonometric polynomial curves with local bias, *J. Comput. Appl. Math.*, **180** (2005), 161–172. https://doi.org/10.1016/j.cam.2004.10.008
21. U. Bashir, M. Abbas, J. Ali, The G^2 and C^2 rational quadratic trigonometric Bézier curve with two shape parameters with applications, *Appl. Math. Comput.*, **219** (2013), 10183–10197. https://doi.org/10.1016/j.amc.2013.03.110
22. L. Yan, X. Han, Q. Zhou, Quadratic hyperbolic Bézier curve and surface (Chinese), *Computer Engineering and Science*, **37** (2015), 162–167.
23. F. Pelosi, R. Farouki, C. Manni, A. Sestini, Geometric Hermite interpolation by spatial Pythagorean-hodograph cubics, *Adv. Comput. Math.*, **22** (2005), 325–352. https://doi.org/10.1007/s10444-003-2599-x
24. R. Ait-Haddou, M. Barton, Constrained multi-degree reduction with respect to Jacobi norms, *Comput. Aided Geom. D.*, **42** (2016), 23–30. https://doi.org/10.1016/j.cagd.2015.12.003
25. C. González, G. Albrecht, M. Paluszny, M. Lentini, Design of C^2 algebraic-trigonometric Pythagorean hodograph splines with shape parameters, *Comput. Appl. Math.*, **37** (2018), 1472–1495. https://doi.org/10.1007/s40314-016-0404-y
26. M. Mazure, Which spaces for design? *Numer. Math.*, **110** (2008), 357–392. https://doi.org/10.1007/s00211-008-0164-8
27. M. Mazure, On a general new class of quasi Chebyshevian splines, *Numer. Algor.*, **58** (2011), 399–438. https://doi.org/10.1007/s11075-011-9461-x
28. M. Mazure, Quasi extended Chebyshev spaces and weight functions, *Numer. Math.*, **118** (2011), 79–108. https://doi.org/10.1007/s00211-010-0312-9

29. T. Bosner, M. Rogin, Variable degree polynomial splines are Chebyshev splines, *Adv. Comput. Math.*, **38** (2013), 383–400. https://doi.org/10.1007/s10444-011-9242-z

30. L. Schumaker, *Spline functions: basic theory*, Cambridge: Cambridge University Press, 2007. https://doi.org/10.1017/CBO9780511618994

31. H. Pottmann, The geometry of Tchebycheffian splines, *Comput. Aided Geom. D.*, **10** (1993), 181–210. https://doi.org/10.1016/0167-8396(93)90036-3

32. M. Mazure, Blossoming: a geometrical approach, *Constr. Approx.*, **15** (1999), 33–68. https://doi.org/10.1007/s003659900096

33. M. Mazure, Blossoming stories, *Numer. Algor.*, **39** (2005), 257–288. https://doi.org/10.1007/s11075-004-3642-9

34. M. Mazure, On a new criterion to decide whether a spline space can be used for design, *BIT Numer. Math.*, **52** (2012), 1009–1034. https://doi.org/10.1007/s10543-012-0390-4

35. J. Peña, *Shape preserving representations in computer-aided geometric design*, New York: Nova Science Publishers, 1999.

36. G. Farin, *Curves and surfaces for computer-aided geometric design: a practical guide*, Boston: Academic Press, 1990. https://doi.org/10.1016/C2009-0-22351-8

37. J. Peña, Shape preserving representations for trigonometric polynomial curves, *Comput. Aided Geom. D.*, **14** (1997), 5–11. https://doi.org/10.1016/s0167-8396(96)00017-9

38. J. Carnicer, J. Peña, Totally positive bases for shape preserving curve design and optimality of B-splines, *Comput. Aided Geom. D.*, **11** (1994), 633–654. https://doi.org/10.1016/0167-8396(94)90056-6

39. L. Gori, F. Pitolli, Totally positive refinable functions with general dilation, *Appl. Numer. Math.*, **112** (2017), 17–26. https://doi.org/10.1016/j.apnum.2016.10.004

AIMS Press